HPLC Characterization of Hydrogenous Polystyrene-block-deuterated polystyrene Utilizing the Isotope Effect

ARTICLE *in* MACROMOLECULES · NOVEMBER 2013

Impact Factor: 5.8 · DOI: 10.1021/ma4018247

CITATIONS
5

READS
30

8 AUTHORS, INCLUDING:

Taihyun Chang
Pohang University of Science and Technology
248 PUBLICATIONS **5,862** CITATIONS
SEE PROFILE

Yutian Zhu
Chinese Academy of Sciences
43 PUBLICATIONS **356** CITATIONS
SEE PROFILE

Yongmei Wang
The University of Memphis
91 PUBLICATIONS **1,455** CITATIONS
SEE PROFILE

Macromolecules

Article

pubs.acs.org/Macromolecules

HPLC Characterization of Hydrogenous Polystyrene-*block*-deuterated polystyrene Utilizing the Isotope Effect

Sanghoon Lee, Hyojoon Lee, Lam Thieu, Youncheol Jeong, and Taihyun Chang*

Division of Advanced Materials Science and Department of Chemistry, Pohang University of Science and Technology (POSTECH), Pohang, 790-784, Korea

Chao Fu and Yutian Zhu*

State Key Laboratory of Polymer Physics and Chemistry, Changchun Institute of Applied Chemistry, Chinese Academy of Sciences, Changchun 130022, People's Republic of China

Yongmei Wang

Department of Chemistry, The University of Memphis, Memphis, Tennessee 38152-3550, Unitied States

ABSTRACT: HPLC elution behavior of isotopically different block copolymers was investigated. A series of three diblock copolymers of hydrogenous polystyrene and deuterated polystyrene (hPS-*b*-dPS), in which the length of hPS-block is fixed at 18 kg/mol and the length of dPS-block is varied from 17 kg/mol to 80 kg/mol, was synthesized and their retention behavior in liquid chromatography at critical condition (LCCC) was investigated using a C18 coated silica stationary phase and a mixed solvent of CH_2Cl_2 and CH_3CN. At this LC separation condition, hPS is retained slightly longer than dPS. The LCCC separations were performed at both LCCC conditions of dPS and hPS established with the same stationary and mobile phases, but at different column temperatures. Since the chromatographic retention difference between dPS and hPS is very small, it was possible to elute the block copolymers at both exclusion and interaction modes at the critical condition of each individual block. We found that the block at its critical condition is not fully "invisible" in both cases. In the LCCC separation at the critical condition of dPS, hPS-*b*-dPS elutes after the injection solvent peak (interaction mode) due to the stronger interaction of the hPS block. Although they have the same hPS block, they do not coelute but elute in the order of decreasing total molecular weight like an elution in exclusion mode. It clearly demonstrates that the dPS block is not "invisible" at the critical condition but influences the retention of the block copolymers. Monte Carlo simulations of the partition coefficient of A-*b*-B into a slit pore were performed to give insight on the elution behavior of A-*b*-B at the critical condition of the B block. The simulation shows that a block under the critical condition influences the retention of the other "visible" block whether the "visible" block is eluted in exclusion or interaction mode. When A is eluted in the interaction mode and B is at its critical condition, the partition coefficient is found to decrease with the increase of the "invisible" B block length, conforming to the observed elution behavior in experiments.

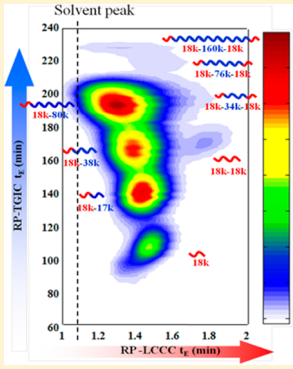

INTRODUCTION

While size exclusion chromatography (SEC) has been a dominant tool for polymer characterization since it was developed almost a half century ago, applications of other chromatographic techniques have been increasing in recent years in response to the growing need of more precise characterization.[1−4] Interaction chromatography (IC) and liquid chromatography at critical condition (LCCC) are representative techniques to complement SEC. In principle, SEC, IC, and LCCC are not entirely different techniques, but these three separation modes can be established with the same chromatographic system by changing either mobile phase or column temperature. Because of the large molecular size of polymers, entropic size exclusion effect always exists together with the enthalpic interaction with the stationary phase in LC separations using porous packing materials. Depending on relative magnitude of exclusion and interaction effect of the polymer molecules while they pass through the porous packing materials, SEC (when exclusion effect dominates the interaction effect, polymers elute before the injection solvent peak with the decreasing order of molecular size), LCCC (when exclusion effect is balanced with the interaction effects, polymers elute near the injection solvent peak independent of molecular size), and IC (when interaction effect dominates the exclusion effect, polymers elute after the injection solvent peak with the increasing order of molecular weight) elution modes

Received: September 2, 2013
Revised: October 20, 2013
Published: November 6, 2013

are observed. These separation modes have their own merits and limitations. Often one separation mode provides information complementary to the other and a coupling of two separation mode to a two-dimensional LC can be far more informative than two independent LC separations.[5−7] Among the three LC separation modes of polymers, LCCC has been used widely for the characterization of block copolymer and functionality in polymers.[4,8−10] At the critical condition of a homopolymer, the homopolymer elute almost independent of molecular weight (MW). If a polymer has an additional difference in its chemical structure such as additional functional groups or other blocks in block copolymers, the retention of the polymer would be largely determined by the additional part.

In this study, we investigated the LCCC retention behavior of block copolymers containing isotopically different blocks. Isotopes are chemically very similar but exhibit characteristic differences which can be effectively utilized in chemical analysis such as in NMR and neutron scattering.[11,12] In addition, albeit it is less expected, isotopes can show a measurable difference in LC retention of polymers.[7,13−15] For example, the contrast in LC retention of hydrogen and deuterium allowed an excellent 2D-LC separation of comb-shaped polystyrene (PS) containing a hydrogenous PS (hPS) backbone and deuterated PS (dPS) branches although the separation mechanism was not fully understood.[7] We would like to elucidate the isotope effect in the separation of the comb-shaped PS from this study. In addition, we would like to critically examine the claim that a block in block copolymers is chromatographically "invisible" at the critical condition of the block. Many of the LCCC characterization of high MW block copolymers have been made for this purpose to measure the MW of the "visible" block by the standard calibration method as in the conventional SEC analysis.[1,2,8,16] Many of these investigations support the applicability of LCCC for the characterization of selected block of block copolymers. On the other hand, we found that a block in PS-*b*-polyisoprene (PI) was not completely "invisible" at the critical condition of its homopolymer, and the retention of the block copolymers is affected to some extent by the length and chain architecture of the "invisible" block under its LCCC condition.[17−19] The effect of the "invisible" block increases as the size of the "invisible" block increases relative to the "visible" block. For example, the retention of a "visible" block of constant block length eluting in the SEC regime gradually increases and the apparent MW of the block decreases as the MW of the "invisible" block increases. This result was supported by a computer simulation study using self-avoiding walk chains.[20]

Since hPS and dPS are nearly identical in their chemical nature, the eluent strength of a solvent for both blocks should be nearly identical. It will eliminate the possible ambiguity on the issue of different solvent quality for different blocks. In addition, it would be possible to elute the block copolymers in both exclusion and interaction modes at the critical condition of each block since the interaction strength of dPS and hPS with the stationary phase should be very similar, too. It will provide us with a very rare opportunity to rigorously examine the chromatographic invisibility in both SEC and IC elution mode of "visible" block. For a pair of different blocks in typical block copolymers, it is only possible to elute block copolymers in SEC mode at the critical condition of the more strongly interacting block.

EXPERIMENTAL SECTION

Preparation of Block Copolymers. Three hPS-*b*-dPS diblock copolymers with a fixed length of hPS block and varying lengths of dPS block were prepared by sequential anionic polymerization of styrene and deuterated (d_8) styrene. Anionic polymerization of the block copolymers was carried out in cyclohexane (Aldrich) at 40 °C under purified Ar atmosphere. Details of the apparatus and the polymerization procedure were reported previously.[21] The styrene (Aldrich) and styrene-d_8 (Alfa Aesar) were first treated with CaH_2 prior to the final purification by stirring with dibutylmagnesium (Aldrich) for 2 h at room temperature before vacuum distillation. An appropriate amount of the initiator, *sec*-butyllithium in hexane (Aldrich), was added to the cyclohexane solvent in the reactor kept at 45 °C, and the polymerization was initiated by adding the purified styrene monomer. After the polymerization of the hPS block for 2 h, the hPS anion solution was transferred by a cannula to three separate reactors which contain precalculated amounts of purified styrene-d_8 monomer according to the target MW. The polymerization of the dPS block was carried out at 45 °C for 3 h. The polymerizations were terminated with degassed isopropanol (Samchun, HPLC grade). As-synthesized hPS-*b*-dPS contains small amounts of the hPS precursor and the coupled product of PS anions as byproducts. For unambiguous LCCC analyses, the byproducts were removed by fractionation using a home-packed prep-column (Nucleosil, 70 × 22 mm, 100 Å, 5 μm) using a THF−hexane mixture (44/56, v/v) as a mobile phase.

SEC Analysis. All polymers used in this study including homopolymer standards and the prepared block copolymers were characterized by SEC/light scattering detection. The specific refractive index increments (d*n*/d*c*) of hPS and dPS were measured in THF as 0.185 and 0.187 mL/g, respectively, and the difference is nearly negligible. Two mixed bed columns (Agilent, Polypore) were used at a column temperature of 40 °C. SEC chromatograms were recorded with a triple detector (Malvern, TDA 300). The solvent was THF (Samchun, HPLC grade) at a flow rate of 0.8 mL/min. Polymer samples for the SEC analysis were dissolved in THF at a concentration of ∼1 mg/mL and the injection volume was 100 μL.

LCCC Analysis. For LCCC analyses, a C18 bonded silica column (Phenomenex, Lunasil C18, 150 × 4.6 mm, 100 Å pore, 5 μm particle) and a mixed eluent of CH_2Cl_2/CH_3CN (57/43, v/v, Samchun, HPLC grade) were used at a flow rate of 0.5 mL/min. Temperature of the column was controlled by circulating fluid from a programmable bath/circulator (Thermo-Haake, C25P) through a homemade column jacket. Sample solutions (∼1 mg/mL) were prepared by dissolving the polymers in a small volume of the corresponding eluent and the injection volume was 100 μL. The chromatograms were recorded by a UV absorption detector (Younglin, UV7300) operating at a wavelength of 260 nm. Homemade hPS and commercial dPS samples (Polymer Source) were used as calibration standards for the analysis of block copolymers.

2D-LC (TGIC × LCCC) Analysis. The 2D-LC analysis was carried out by combining a temperature gradient IC (TGIC) and an LCCC to separate hPS-*b*-dPS according to the total MW of block copolymers and to separate hPS-*b*-dPS according to the hPS content only, respectively. The same stationary (Phenomenex, Lunasil C18, 5 μm, 100 Å pore, 150 × 4.6 mm) and mobile phases (CH_2Cl_2/CH_3CN, Samchun, HPLC grade, 57/43, v/v) were used for both TGIC and LCCC. The only difference was the column temperature. The TGIC column temperature was maintained 10 °C for 30 min, varied from 10 to 20 °C over 30 min and from 20 to 35 °C over 180 min in two linear segments. Afterward, the column temperature was maintained at 35 °C. The flow rate in the first-D TGIC was set at 0.05 mL/min in order to synchronize with the second-D LCCC separations. The second-D flow rate was 1.5 mL/min at a column temperature of 33.6 °C, which is the critical temperature of dPS. The second-D LCCC run was repeated every 2 min while the first-D TGIC eluted the effluent to fill up a 100 μL storage loop. Total analysis time was about 4 h. Two HPLC pumps (pump 1, Shimadzu, LC-20AD; pump 2, Bischoff compact pump 2250) and two UV detectors (Younglin, UV7300) were used. The two LC systems were connected via electronically

dx.doi.org/10.1021/ma4018247 | *Macromolecules* 2013, 46, 9114−9121

controlled 10-port 2-position switching valves (Alltech, SelectPro) equipped with two 100 μL storage loops. Control of the switching valves and data acquisition were done by homemade computer software. The 2D-LC system is similar to the one reported previously.[22]

Monte Carlo Simulation. In this study, the A-*b*-B block copolymer chains have been modeled as both self-avoiding walk (SAW) chains and random walk (RW) chains in a simple cubic lattice with dimensions of $250a \times 250a \times 30a$ along the *X*, *Y* and *Z* directions where *a* represents the lattice unit length. The A block is the "visible" block, while the B block is the "invisible" block. When A block is in the IC mode and B block is at the critical condition, the modeled A-*b*-B block copolymer corresponds to the hPS-*b*-dPS diblock copolymer in the experiments. Periodic boundary conditions are applied in the *X* and *Y* directions. In the Z direction, however, there are two impenetrable walls at the $Z = a$ and $Z = 30a$, representing the slit pore surfaces. The dimension along the Z direction has also been varied to represent different pore size.

The standard chemical potential of the polymer chain in the slit, μ_{in}^0, is calculated with biased chain insertion method. Detailed description for the calculation can be found in a large amount of the previous simulation studies.[23−28] Briefly, we first randomly select one site within the slit pore and place the first polymer bead on it. The remaining polymer beads are then grown using the biased chain insertion method.[29] When the polymer beads are on the plates of $Z = 2a$ and $Z = 29a$, they are considered to be adsorbed on the pore surfaces. For all the adsorbed polymer beads, the polymer-surface interaction energies, ε_w(A) and ε_w(B), are applied for A and B monomers, respectively. In order to match the experimental samples, we set the length of A as 40 and vary the length of B from 0 to 180. When length of B is zero, the modeled chain becomes the homo-A. The partition coefficient *K* can be obtained by the equation of $\ln K = -(\mu_{in}^0 - \mu^0{}_{bulk})$, where $\mu^0{}_{bulk}$ is the standard chemical potential of the chain in the bulk solution in a cubic lattice of dimension $100a \times 100a \times 100a$ with periodic boundary conditions applied in all three directions.

RESULTS AND DISCUSSION

Figure 1a shows the SEC chromatograms of the as-prepared polymers. Since SEC separates polymers according to the chain size in a good solvent, isotopic content affects the SEC retention little. The precursor hPS contains a small amount of coupled product eluting earlier than the major product. hPS-*b*-dPS samples clearly show progressively increasing MW (decreasing elution time, t_E) from the sample 1 to 3. All samples contain a finite amount of inadvertently terminated hPS precursor eluting at $t_E \sim 18$ min as well as a small amount of coupled product of each, which appears as a small peak eluting earlier than the main peak.[30]

As-prepared block copolymers were fractionated to make the LCCC analysis free from the interference of byproducts. The byproducts were removed by normal phase liquid chromatography (NPLC) fractionation under isothermal condition. The NPLC separation using bare silica stationary phase is known to be less sensitive to the isotopic content of the polymer so that the block copolymers were separated according to the molecular weight more or less independent of the isotopic content.[7,14] Figure 1b displays the NPLC chromatograms of the three as-prepared hPS-*b*-dPS. To optimize the fractionation, the column temperature was set differently for the sample 1, 2, and 3 at 5, 15, and 23 °C, respectively. Therefore, the relative elution time of the three block copolymers cannot be compared directly. The column temperatures were chosen to elute the block polymers (main broad peaks) quickly while resolving them well from the hPS precursor (labeled with arrows) eluting earlier than hPS-*b*-dPS. The small peak eluting at $t_E \sim 11$ min is

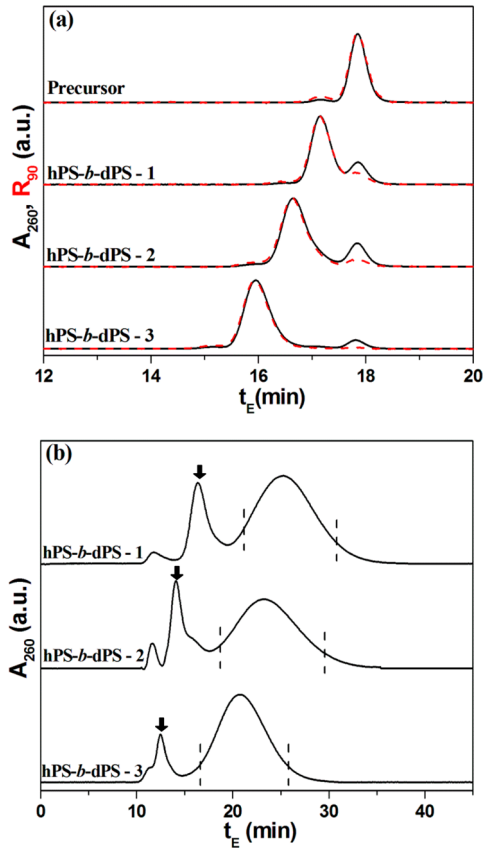

Figure 1. (a) SEC chromatograms of the as-prepared hPS precursor and hPS-*b*-dPS recorded by a UV absorption (black solid line) and a light scattering (red dashed line) detector. Separation condition: two mixed bed columns (Agilent, Polypore), THF eluent at a column temperature of 40 °C. Flow rate: 0.8 mL/min. (b) NPLC chromatograms of as-prepared hPS-*b*-dPS recorded by a UV absorption detector for fractionation. Separation condition: a home-packed semiprep column (Nucleosil, 70 × 20 mm, 100 Å, 5 μm). Eluent: THF/*n*-hexane mixture (44/56, v/v). Flow rate: 2 mL/min. Column temperatures are fixed at 5, 15, and 23 °C for the sample 1, 2, and 3, respectively. Dashed vertical lines indicate the elution time range where the fractions were collected.

the injection solvent peak. Peaks of the coupled products are difficult to identify since the amount is small and the peak is broadened at longer elution time. The portions between the dashed vertical lines were collected for the LCCC analysis. Fractionated hPS-*b*-dPS and the precursor hPS were characterized by SEC as displayed in Figure 2. All hPS-*b*-dPS exhibit a narrow and unimodal elution peak and it is clear that hPS precursors are removed well although trace amounts of the coupled products are still left. The MWs of the fractionated polymers were determined by light scattering detection and the results are summarized in Table 1. The MW of dPS block was calculated from the total MW and the hPS precursor MW.

Analysis of hPS-*b*-dPS at the Critical Condition of Each Block. Figure 3a shows the LCCC chromatograms of hPS standards of three different MW (11K, 27K, and 48K). They coelute quite precisely a little after the injection solvent peak position (vertical dashed line). The critical condition of hPS was established at 40 °C. At the critical condition of hPS, hPS-*b*-dPS eluted in the decreasing order of MW before the solvent peak as displayed in Figure 3b. As expected, the "visible" dPS block interacts less than the "invisible" hPS block

dx.doi.org/10.1021/ma4018247 | *Macromolecules* 2013, 46, 9114−9121

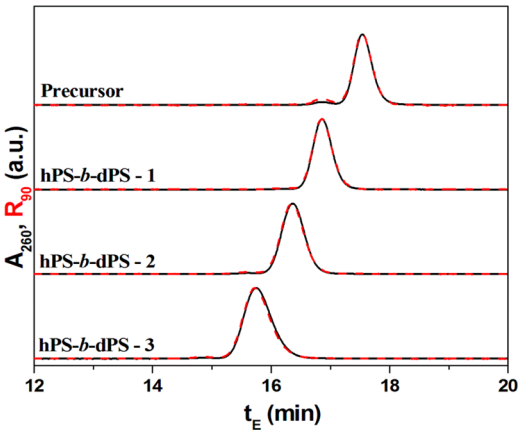

Figure 2. SEC chromatograms of the hPS precursor and fractionated hPS-*b*-dPS recorded by a UV absorption (black solid line) and light scattering (red dashed line) detectors. Separation condition: Two mixed bed columns (Agilent, polypore), THF eluent at a column temperature of 40 °C. Flow rate was 0.8 mL/min.

Table 1. Molecular Characteristics of hPS Precursor and hPS-*b*-dPS

	M_p	$M_{p,hPS} - M_{p,dPS}$ (M_w/M_n)
hPS precursor	17 800	17 800−0 (1.01)
hPS-*b*-dPS-1	34 700	17 800−16 900 (1.01)
hPS-*b*-dPS-2	55 500	17 800−37 700 (1.01)
hPS-*b*-dPS-3	98 000	17 800−80 200 (1.01)

Determined by SEC/Light scattering method. M_p: peak MW.

and the block copolymers elute in the SEC mode. The weaker interaction strength of dPS than hPS with the C18 coated silica packing materials was reported previously.[14] The calibration curve obtained with homo-dPS is also shown. The MW of the "visible" dPS block was determined with respect to the calibration curve. We will be back to the issue later.

Figure 4a shows the chromatograms of three different MW dPS standards (6K, 25K, and 46K) at the critical condition of dPS. They again coelute quite precisely, a little after the injection solvent peak position (dashed vertical line). The critical condition for dPS was established at 33.6 °C, a lower column temperature than hPS, 40 °C. The lower critical condition temperature of dPS reflects that dPS interacts with the C18 stationary phase less strongly than hPS. At this critical condition, dPS block is supposed to become "invisible" and the hPS-*b*-dPS are to be retained by the "visible" hPS block. Figure 4b displays the LCCC chromatograms of the three hPS-*b*-dPS and hPS precursor at the critical condition of dPS. As expected, three hPS-*b*-dPS as well as hPS precursor elute after the injection solvent peak (vertical dashed line) since the "visible" hPS is retained more strongly than dPS at this separation condition. They did not coelute, however, despite their identical hPS block length. They elute in the decreasing order of total MW as displayed in Figure 4b: High MW polymer elutes earlier than low MW polymer like the sequence in an SEC elution even though they elute after the elution of the injection solvent, i.e., in the IC mode. This type of peculiar retention behavior has been found in the entropy-driven chromatography (hydrophobic interaction chromatography) separations before.[31−33] To our knowledge, such an inverse MW order elution in an enthalpy-driven interaction chromatography separation has never been observed. To elucidate the

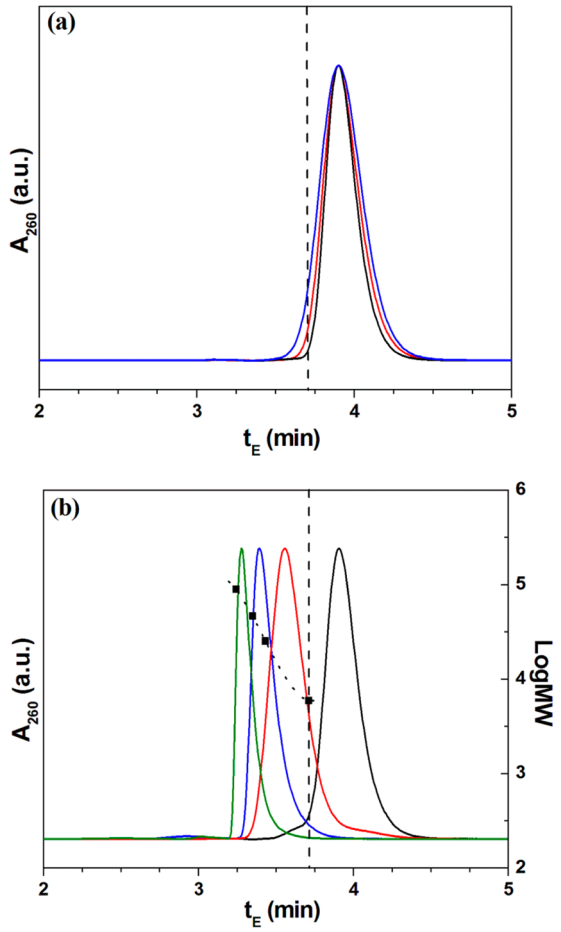

Figure 3. (a) Elution behavior of hPS standards (11K, 27K, 48K) at the critical condition. Column: Lunasil C18, 100 Å, 150 × 4.6 mm at 40 °C. Eluent: CH_2Cl_2/CH_3CN (57/43, v/v). (b) Elution behavior of hPS-*b*-dPS and hPS precursor at the critical condition of hPS. (From left, MW of dPS block = 80.2K, 37.7K, 16.9K; hPS precursor). The calibration curves of dPS made with dPS standards (M_p: 89.4K, 46.4K, 25.3K, 5.9K) is also shown. The solvent peak position is marked with a vertical dashed line.

elution mechanism of this peculiar chromatographic elution, we carried out a simulation study as described later.

Also shown in Figure 3b and 4b are the calibration curves drawn from the retention of dPS and hPS standards, respectively. If a block under critical condition becomes truly "invisible", MW of the "visible" block can be determined according to the calibration curve of the homopolymers.[4] In most cases, such LCCC characterizations of the "visible" blocks of block copolymers have been done in the SEC mode. Block copolymers with chemically (not isotopically) different blocks cannot be eluted at an LCCC condition of the more weakly interacting block since interaction of the other (more strongly interacting) block with the stationary phase makes the polymer retained too long. In the IC separation of polymers, the retention of polymers usually need to be controlled by solvent gradient or temperature gradient elution since the retention time increases exponentially with MW. Since an LCCC separation is an isocratic and isothermal elution process, it is difficult even for a block of very weak interaction to be eluted over a wide MW range. Therefore, it has been possible to elute block copolymers in the IC elution mode only for LCCC characterization of very short blocks.[17,34] In this regard, the

dx.doi.org/10.1021/ma4018247 | *Macromolecules* 2013, 46, 9114−9121

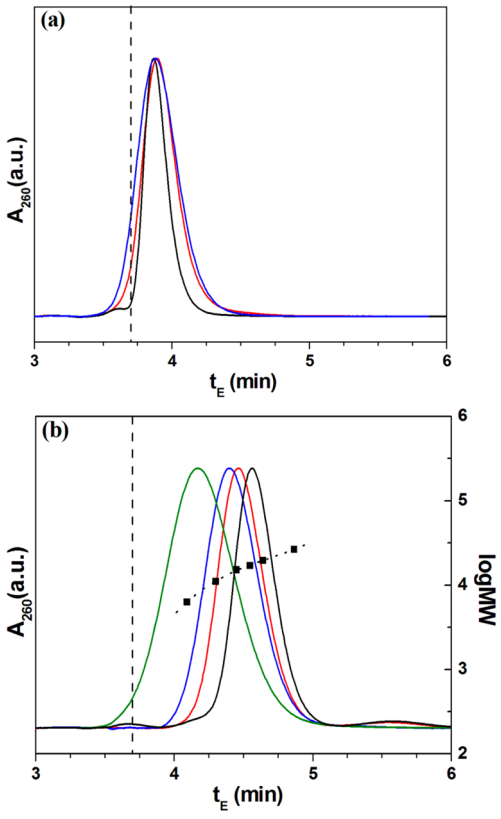

Figure 4. (a) Elution behavior of dPS standards (6K, 25K, 46K) at the critical condition of dPS. Column: Lunasil C18; 100 Å; 150 × 4.6 mm at 33.6 °C. Eluent: CH_2Cl_2/CH_3CN (57/43, v/v). (b) Elution behavior of hPS-*b*-dPS and hPS precursor at the critical condition of dPS. (From left, MW of dPS = 80.2K, 37.7K, 16.9K; hPS precursor). The calibration curves of hPS made with hPS standards (M_p: 6.3K, 15.3K, 16.9K, 19.6K, 25.7K, 47.5K) is also shown. The solvent peak position is marked with a vertical dashed line.

hPS-*b*-dPS samples provide us with a very unique opportunity that an LCCC characterization of a block can be done in the IC elution mode since the interaction strengths of hPS and dPS are almost identical (but distinguishable) so that block copolymers with different block length can be eluted by an isocratic/isothermal LCCC elution. Thus, we were able to characterize both blocks of hPS-*b*-dPS by LCCC characterization in both SEC and IC modes and the results are summarized in Table 2.

Table 2. LCCC Characterization hPS-*b*-dPS: (a) Characterization of dPS Block at the Critical Condition of hPS Block; (b) Characterization Results of hPS Block at the Critical Condition of dPS Block

	$M_{p,dPS}$	
a	expected M_p	measured M_p at CC of hPS (% error[a])
hPS-*b*-dPS-1	16 900	10 100 (40.2)
hPS-*b*-dPS-2	37 700	33 500 (11.4)
hPS-*b*-dPS-3	80 200	74 800 (6.7)
	$M_{p,hPS}$	
b	expected M_p	measured M_p at CC Of dPS (% error[a])
hPS-*b*-dPS-1	17 800	15 600 (12.4)
hPS-*b*-dPS-2	17 800	14 000 (21.3)
hPS-*b*-dPS-3	17 800	8 200 (53.9)

[a]Error: $100(M_{p,expected} - M_{p,LCCC})/M_{p,expected}$

The M_p in Table 2 is the peak MW determined by calibration with respect to the homo-hPS and dPS standard samples. The M_p values measured at both critical conditions show significant deviation from the true value confirming that the blocks in critical condition is not completely "invisible". The trend of the relative errors in the SEC mode elution is consistent with the previous results of PS-*b*-PI that the relative error increases as the size of the "visible" block (dPS in this case) relative to "invisible" block (hPS in this case) decreases.[17] The same trend was also found in the IC mode elution. The relative error increases as the dPS block (in this case "invisible block") gets longer. Therefore, the smallest relative error was found in PS-*b*-dPS-1 in which relative size of hPS block ("visible" block) is the largest among the three block copolymers.

Monte Carlo Simulation Study. The influence of the "invisible" block on the LCCC characterization of the block copolymers has been examined earlier both in experiments and simulations.[17−20,35] But these earlier studies covered only the case where the "visible" block eluted in the SEC mode. Data in Figure 3b and Table 2a in the current study reflects the known phenomenon: that is the presence of the invisible block leads to an underestimate of the block length of the "visible" block when the visible block is eluted in the SEC mode. The new and "surprising" results emerged in the current study are the data in Figure 4b and Table 2b where the visible block is eluted in the interactive mode. Here we performed Monte Carlo simulations to shed lights on the observed experimental data.

Both the SAW model and RW model were used in the current work to clarify the effect of "invisible" block on LCCC analysis of A-*b*-B block copolymer. The critical conditions for the RW and SAW models are at $\varepsilon_w = -0.18232$ and $\varepsilon_w = -0.276$, respectively, as determined earlier.[10,24,28] In the simulation, A will be the visible block and B will be the invisible block by setting ε_w(B) at the critical condition. When ε_w(B) at the critical condition and ε_w(A) is in a interactive mode, the simulation parameters correspond to the experimental condition in Figure 4b. Figure 5 presents the dependence of K(A-*b*-B)/K(A) on the length of the "invisible" B block, N(B), where K(A-*b*-B) and K(A) are the partition coefficients of A-*b*-B diblock and A homopolymer when the length of A is fixed at 40. The figure includes the point when N(B) = 0 corresponding to homo-A at which K(A-*b*-B)/K(A) = 1.0. Deviation of K(A-*b*-B)/K(A) from one means that the partition coefficient of diblock, K(A-*b*-B), is not the same as the homopolymer, K(A), which implies that the "invisible" B block exerts an influence on K(A-*b*-B). For the RW case, the data forms a fanlike pattern as displayed in Figure 5a. When A is in the SEC mode [ε_w(A) < ε_w(B)], K(A-*b*-B)/K(A) > 1. The diblock is retained longer than the homo-A, and the longer the "invisible" block, the more the deviation. This is the same phenomenon reported in the previous experimental and theoretical results.[17,20] On the other hand, when the visible A block elutes in the IC mode, we see that K(A-*b*-B)/K(A) < 1. Moreover, an increase in the invisible B block results a decrease in the K(A-*b*-B). This is exactly the same phenomenon observed in experiments shown in Figure 4b and Table 2b. The data with the SAW model provides a similar pattern but with some complications. When the "visible" A block is in the IC mode, K(A-*b*-B) does not immediately become smaller than K(A), although the decrease in K(A-*b*-B) with the increase in the "invisible" block length is still seen (see curves with ε_w(A) = −0.34 and -0.36 in Figure 5b). With a further increase in the interaction energy of the "visible" block, one observes the same

dx.doi.org/10.1021/ma4018247 | *Macromolecules* 2013, 46, 9114−9121

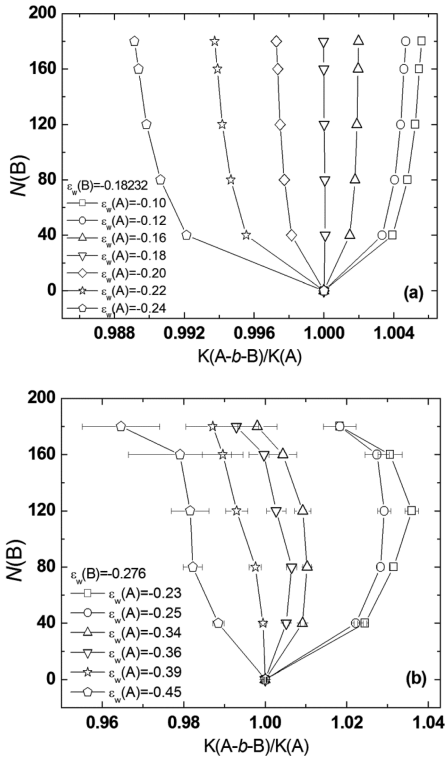

Figure 5. Plot of B block length N(B) vs K(A-*b*-B)/K(A) at the critical condition of B block. (a) ε_w(B) = −0.18232 and (b) ε_w(B) = −0.276. The length of visible A block is fixed as 40. The interaction of A block with the surface ε_w(A) is varied from SEC mode to IC mode. (a) RW chain model: ε_w(A)= −0.10, −0.12, −0.16 correspond to the SEC mode and ε_w(A) = −0.20, −0.22, and −0.24 correspond to the IC mode. (b) SAW chain model: ε_w(A) = −0.23, −0.25 correspond to the SEC mode and ε_w(A)= −0.34, −0.36, −0.39, and −0.45 correspond to the IC mode.

pattern as in RW model, K(A-*b*-B)/K(A) < 1 and K(A-*b*-B) decreases with an increase in B length.

From these data, we can therefore conclude that the influence of the "invisible" B block on the retention of a diblock copolymer is present even in the RW model. The excluded volume interaction accounted for in the SAW adds only as a secondary effect. Previous theoretical discussions using the Gaussian chain model suggested that when B block is in the critical condition, the partition coefficient of the diblock K(A-*b*-B) equals to K(A).[36] Here we see that this is not strictly true. Even in the RW model there is small deviation between K(A-*b*-B) from K(A) whether A is in the SEC mode or IC mode. The simulations with RW model alone could account for the previous known experimental data and the new experimental data in Figure 4b.

We think that the influence of the "invisible" block on the retention of a diblock copolymer comes from the chain connectivity. In a diblock copolymer such as the A-*b*-B, the A block and the B block are connected via the covalent bond at the joint. When the interaction of the two blocks with the surface is not the same, they influence each other. Whichever the block interacts less with the surface than the other block, that block will pull the other block away from the surface and vice versa. However, since we are comparing the retention of the diblock K(A-*b*-B) with the retention of homopolymer K(A), it is easier to understand the results when one thinks how the B block exerts its influence on the A block. In the current study corresponding to the condition in Figure 4b, the dPS is the invisible B block at the critical condition and hPS is the visible A block in the IC mode. The visible hPS (the A block) is adsorbed onto the column surface more than the invisible dPS block (the B block). Therefore, dPS block tends to pull the hPS block away from the surface, resulting a decrease of K(A-*g*-B) from K(A). Also, in Figure 4b and Table 2b, the length of the invisible B block (dPS) is increasing and the length of visible hPS block is fixed. As a result, the "pulling" effect of invisible dPS block on the visible hPS block becomes more and more significant, which makes the partition coefficient for K(hPS-*b*-dPS) smaller than K(hPS), resulting more discrepancy between measured and expected molecular weight of the visible hPS block. In another situation corresponding to experimental condition in Figure 4a and Table 2a, the visible A block is the dPS in the SEC mode, and the invisible B block is the hPS in the critical condition. In this case, the visible dPS is adsorbed less on the surface than the invisible hPS. One can therefore imagine invisible hPS will anchor the visible dPS closer to the wall gaining additional enthalpic interaction. As a result, K(A-*b*-B) > K(A), as observed here in simulations. Moreover, in Table 2a, the length of visible dPS block is increasing while the length of the invisible hPS block is fixed. Therefore, the anchoring effect of hPS on dPS in this case will diminish as the visible dPS length increases, resulting a smaller discrepancy between the two molecular weights.

With the above notion, we can also expect the following: (1) the deviation between K(A-*b*-B) from K(A), characterized by the ratio K(A-*b*-B)/K(A), will be less if the slit width increases; (2) the deviation between K(A-*b*-B) from K(A) will be less if A length increases. In the first case, when the slit width increases, the chain less likely interacts with the surface. Any of these pulling or anchoring effects of the "invisible" block on the "visible" block will be reduced. Data in Figure 6 confirms such expectation where the slit width is varied from 20*a* to 50*a*. As the slit width increases, K(A-*b*-B)/K(A) gets closer to the ideal LCCC elution behavior, K(A-*b*-B)/K(A) =1.0 in both cases that the "visible" A block is in the SEC mode or the IC mode. In the second case, when A length increases, the pulling effect from the "invisible" B block will also be less since A block is

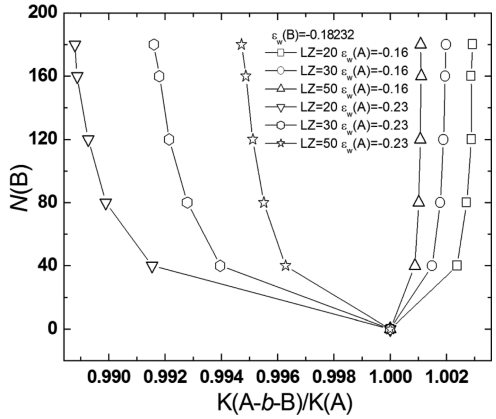

Figure 6. Plot of B block length N(B) vs K(A-*b*-B)/K(A) at the critical condition of B block (ε_w(B) = −0.18232, RW model). The length of A block is fixed as 40. The interaction of A is set as ε_w(A) = −0.16 or ε_w(A) = −0.23, which corresponds the SEC mode and the IC mode, respectively. The width of the lattice box (LZ) is varied from 20*a* to 50*a*.

dx.doi.org/10.1021/ma4018247 | *Macromolecules* 2013, 46, 9114−9121

larger and is not so easily influenced by the B block. This prediction is confirmed by results in earlier studies when the visible block was eluted in the SEC mode.[17,18,20] Comparing data in Figure 5a and Figure 5b, one can see that excluded volume interaction accounted for in the SAW model adds an additional effect on top of the chain connectivity. Notably, when the visible block is eluted in the SEC mode, K(A-*b*-B) will first increase with the increase of "invisible" B block but then decrease upon further increase. However, it is not clear if such a phenomenon is observable in experiments. The excluded volume interaction will be more pronounced for branched or star polymers and maybe observable in these systems.

2D-LC Separation of hPS-*b*-dPS Mixture. To understand the elution behavior of hPS-*b*-dPS near the critical conditions better, we carried out a 2D-LC separation by combining TGIC (separating the block copolymer mainly by MW) and LCCC (separating the block copolymer mainly by MW of the "visible" block). TGIC separation of hPS-*b*-dPS according to the total MW could be done more efficiently under NPLC condition than reversed-phase (RP) LC.[7,14] Nonetheless, RP-TGIC was used for the first-D LC since the use of an identical mobile phase in both LC separations prevents the problems associated with the solvent compatibility.[5,7,37] We found an RP-TGIC separation condition to separate them according to MW reasonably well. Figure 7 shows an RP-TGIC chromatogram of

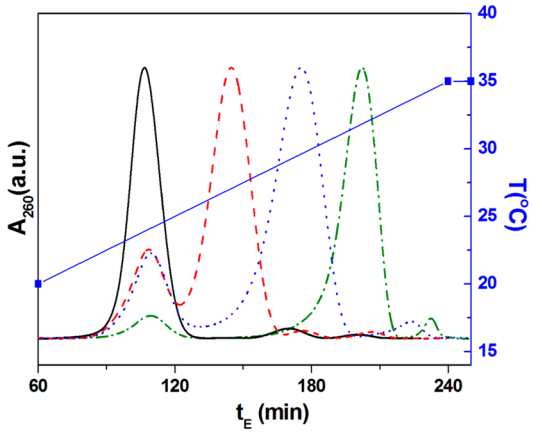

Figure 7. RP-TGIC chromatograms of the as-prepared hPS-*b*-dPS and the hPS precursor (black-solid line, hPS precursor; red-dashed line, hPS-*b*-dPS-1; blue-dotted line, hPS-*b*-dPS-2; green-dash dot line, hPS-*b*-dPS-3). Column: Lunasil C18, 100 Å, 5 μm, 150 × 4.6 mm. Eluent: CH_2Cl_2/CH_3CN (57/43, v/v) at a flow rate of 0.05 mL/min. Temperature program is also shown in the plot.

the as-prepared hPS-*b*-dPS samples together with the hPS precursor. The TGIC separation used the same stationary and mobile phase as in the previous LCCC separations except that the column temperature was varied during the elution. The column temperature was lower than the critical temperatures of both hPS and dPS blocks (i.e., interaction condition of both blocks) so that it separates the hPS-*b*-dPS according to the total MW. Column temperature was linearly increased from 20 to 35 °C in 180 min as shown in Figure 7. The overlay of the TGIC chromatograms of the four polymers shows that they are separated reasonably well according to the total MW of the polymers. The hPS precursor elutes at t_E = 110 min and its coupled product elutes as a weak peak at t_E = 170 min. The three hPS-*b*-dPS elute at t_E = 130 min ~220 min in the increasing order of total MW. All three block copolymers contains a small amount of hPS precursor eluting at t_E = 110 min and their own coupled products eluting after the main peak.

The flow rate of first-D LC needs to be synchronized with the second-D LC analysis. In a comprehensive 2D-LC analysis, a second-D LCCC separation should be completed during a sample storage loop is filled with the first-D TGIC effluent. Then, the 2D-LC chromatogram is essentially an overlay of multiple second-D LC chromatograms and the 2D-LC analysis time is the product of the second-D LC analysis time and the number of the second-D LC chromatograms taken. In this analysis, the time required for the second-D LCCC separation was 2 min. Therefore, during the 2 min, the first-D RP-TGIC separation elutes 100 μL at a flow rate of 0.05 mL/min to fill up the 100 μL loop and it is transferred to the second-D column later. Figure 8 shows a contour plot of RP-TGIC × LCCC 2D-

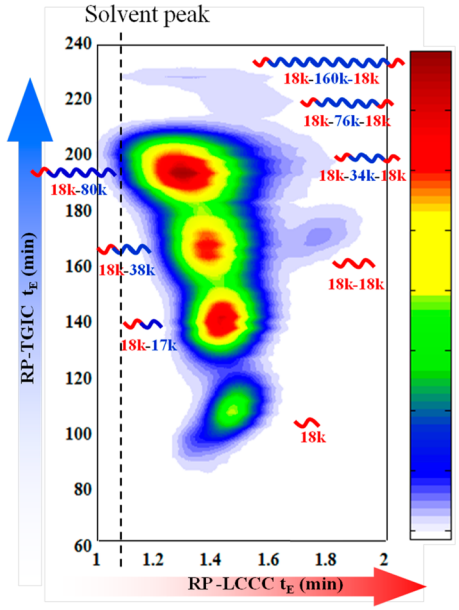

Figure 8. RP-TGIC × LCCC 2D-LC chromatogram of a mixture of three as-prepared hPS-*b*-dPS. The same stationary phase (Lunasil C18, 100 Å, 5 μm, 150 × 4.6 mm) and mobile phase (CH_2Cl_2/CH_3CN, 57/43, v/v) were used for both first-D and second-D LC. For the first-D TGIC, flow rate was 0.05 mL/min and the temperature program was the same as of Figure 6. For the second-D LCCC, flow rate was 1.5 mL/min at a column temperature of 33.6 °C. The vertical dashed line indicates the elution time of the solvent peak in the second-D LCCC.

LC chromatogram of a mixture of the three as-prepared hPS-*b*-dPS. The first-D TGIC is essentially the same as the one shown in Figure 8. In the second-D LCCC, flow rate was 1.5 mL/min at a column temperature of 33.6 °C, which is the critical condition of dPS. The vertical dashed line indicates the elution time of the solvent peak in the second-D LCCC. In this 2D map, a lot more details of the block copolymer mixture are revealed. All side products together with the main polymer species can be identified as labeled in the chromatogram. It is clearly shown that the LCCC retention decreases as MW of the dPS block increases. This exactly resembles the 2D-LC chromatogram of the comb-shaped PS reported earlier.[7] The comb PS must have been separated under the similar separation mechanism at near the LCCC condition of the dPS branches.

In summary, using hPS-*b*-dPS diblock copolymers, we have demonstrated that LCCC separations in both IC and SEC

dx.doi.org/10.1021/ma4018247 | *Macromolecules* 2013, 46, 9114–9121

modes are possible at the critical condition of each block by simply changing the column temperature. We confirmed that a block of critical condition is not perfectly "invisible" and the effect of the "invisible" block caused the size-exclusion type separation of the block copolymers in the IC mode elution. Monte Carlo simulations with SAW and RW models confirm the possibility of such elution behavior in the IC mode. We could achieve an excellent 2D-LC separation of the hPS-*b*-dPS mixture by combining TGIC and LCCC. The 2D-LC combination of IC and LCCC is quite handy since there is no solvent compatibility problem.

AUTHOR INFORMATION

Corresponding Authors

*(T.C.) Telephone: +82-54-279-2787. FAX: +82-54-279-3399. E-mail: tc@postech.ac.kr.

*(Y.Z.) Telephone: +86-43185262866. FAX: +86-43185262126. E-mail: ytzhu@ciac.ac.cn.

Notes

The authors declare no competing financial interest.

ACKNOWLEDGMENTS

We acknowledge the supports from NRF-Korea (R31-10059, 2008-0062045 and 2012R1A2A2A01015148) and the National Natural Science Foundation of China for Youth Science Funds (21104083)

REFERENCES

(1) Chang, T. *Adv. Polym. Sci.* **2003**, *1*, 1−60.

(2) Berek, D. *Macromol. Symp.* **1996**, *110* (1), 33−56.

(3) Chang, T.; Lee, H. C.; Lee, W.; Park, S.; Ko, C. *Macromol. Chem. Phys.* **1999**, *200* (10), 2188−2204.

(4) Pasch, H.; Trathnigg, B., *HPLC of Polymers*; Springer Verlag; Berlin, 1999.

(5) Im, K.; Park, H.-W.; Kim, Y.; Chung, B.; Ree, M.; Chang, T. *Anal. Chem.* **2007**, *79* (3), 1067−1072.

(6) Berek, D. *Anal. Bioanal. Chem.* **2010**, *396* (1), 421−441.

(7) Ahn, S.; Im, K.; Chang, T.; Chambon, P.; Fernyhough, C. M. *Anal. Chem.* **2011**, *83* (11), 4237−4242.

(8) Pasch, H. *Adv. Polym. Sci.* **1997**, *128*, 1−45.

(9) Macko, T.; Hunkeler, D. *Adv. Polym. Sci.* **2003**, *2*, 62−136.

(10) Im, K.; Park, H. W.; Kim, Y.; Ahn, S.; Chang, T.; Lee, K.; Lee, H. J.; Ziebarth, J.; Wang, Y. *Macromolecules* **2008**, *41* (9), 3375−3383.

(11) Higgins, J.; Benoit, H., *Polymers and Neutron Scattering*; Oxford University Press: Cary, NC, 1997.

(12) Cotton, J. P.; Nierlich, M.; Boue, F.; Daoud, M.; Farnoux, B.; Jannink, G.; Duplessix, R.; Picot, C. *J. Chem. Phys.* **1976**, *65* (3), 1101−1108.

(13) Kayillo, S.; Gray, M. J.; Andrew Shalliker, R.; Dennis, G. R. *J. Chromatogr. A* **2005**, *1073* (1−2), 83−86.

(14) Kim, Y.; Ahn, S.; Chang, T. *Anal. Chem.* **2010**, *82* (4), 1509−1514.

(15) Sinha, P.; Harding, G. W.; Maiko, K.; Hiller, W.; Pasch, H. *J. Chromatogr. A* **2012**, *1265*, 95−104.

(16) Falkenhagen, J.; Much, H.; Stauf, W.; Müller, A. H. E. *Macromolecules* **2000**, *33* (10), 3687−3693.

(17) Lee, W.; Cho, D.; Chang, T.; Hanley, K. J.; Lodge, T. P. *Macromolecules* **2001**, *34* (7), 2353−2358.

(18) Lee, W.; Park, S.; Chang, T. *Anal. Chem.* **2001**, *73* (16), 3884−3889.

(19) Park, I.; Park, S.; Cho, D.; Chang, T.; Kim, E.; Lee, K.; Kim, Y. J. *Macromolecules* **2003**, *36* (22), 8539−8543.

(20) Jiang, W.; Khan, S.; Wang, Y. *Macromolecules* **2005**, *38* (17), 7514−7520.

(21) Kwon, K.; Lee, W.; Cho, D.; Chang, T. *Korea Polym. J.* **1999**, *7* (5), 321−324.

(22) Im, K.; Kim, Y.; Chang, T.; Lee, K.; Choi, N. *J. Chromatogr. A* **2006**, *1103* (2), 235−242.

(23) Wang, Y. M.; Teraoka, I. *Macromolecules* **2000**, *33* (9), 3478−3484.

(24) Gong, Y.; Wang, Y. *Macromolecules* **2002**, *35* (19), 7492−7498.

(25) Orelli, S.; Jiang, W.; Wang, Y. *Macromolecules* **2004**, *37* (26), 10073−10078.

(26) Ziebarth, J. D.; Wang, Y. M.; Polotsky, A.; Luo, M. B. *Macromolecules* **2007**, *40* (9), 3498−3504.

(27) Zhu, Y. T.; Ziebarth, J.; Macko, T.; Wang, Y. M. *Macromolecules* **2010**, *43* (13), 5888−5895.

(28) Zhu, Y. T.; Ziebarth, J. D.; Wang, Y. M. *Polymer* **2011**, *52* (14), 3219−3225.

(29) Frenkel, D.; Smit, B., *Understanding Molecular Simulations: From Algorithms to Applications*; Academic Press: New York, 2002.

(30) Park, S.; Cho, D.; Ryu, J.; Kwon, K.; Chang, T.; Park, J. *J. Chromatogr. A* **2002**, *958* (1−2), 183−189.

(31) Trathnigg, B.; Gorbunov, A. *J. Chromatogr. A* **2001**, *910* (2), 207−216.

(32) Cho, D.; Hong, J.; Park, S.; Chang, T. *J. Chromatogr. A* **2003**, *986* (2), 199−206.

(33) Cho, D.; Park, S.; Hong, J.; Chang, T. *J. Chromatogr. A* **2003**, *986* (2), 191−198.

(34) Lee, H.; Lee, W.; Chang, T.; Choi, S.; Lee, D.; Ji, H.; Nonidez, W. K.; Mays, J. W. *Macromolecules* **1999**, *32* (12), 4143−4146.

(35) Yang, X. P.; Zhu, Y. T.; Wang, Y. M. *Polymer* **2013**, *54* (14), 3730−3736.

(36) Gorbunov, A. A.; Vakhrushev, A. V. *J. Chromatogr. A* **2005**, *1064* (2), 169−181.

(37) Jiang, X.; van der Horst, A.; Schoenmakers, P. J. *J. Chromatogr. A* **2002**, *982* (1), 55−68.